

Human Neuroglobin Functions as an Oxidative Stress-responsive Sensor for Neuroprotection*

Received for publication, April 17, 2012, and in revised form, July 7, 2012. Published, JBC Papers in Press, July 11, 2012, DOI 10.1074/jbc.M112.373381

Seiji Watanabe¹, Nozomu Takahashi, Hiroyuki Uchida, and Keisuke Wakasugi²

From the Department of Life Sciences, Graduate School of Arts and Sciences, The University of Tokyo, 3-8-1 Komaba, Meguro-ku, Tokyo 153-8902, Japan

Background: Mammalian neuroglobin (Ngb) is involved in neuroprotection under oxidative stress conditions.

Results: Only under oxidative stress, human Ngb was recruited to lipid rafts by interacting with flotillin-1 and suppressed the activation of $G\alpha_{i/o}$ by acting as its guanine nucleotide dissociation inhibitor.

Conclusion: Human Ngb acts as an intracellular oxidative stress-responsive sensor to protect against cell death.

Significance: The neuroprotective mechanism of human Ngb was revealed.

Mammalian neuroglobin (Ngb) protects neuronal cells under conditions of oxidative stress. The mechanism underlying this function is only partly understood. Here, we report that human Ngb exists in lipid rafts only during oxidative stress and that lipid rafts are crucial for neuroprotection by Ngb. The ferrous oxygen-bound form of Ngb, which exists under normoxia, is converted to the ferric bis-His conformation during oxidative stress, inducing large tertiary structural changes. We clarified that ferric bis-His Ngb, but not ferrous ligand-bound Ngb, specifically binds to flotillin-1, a lipid raft microdomain-associated protein, as well as to α -subunits of heterotrimeric G proteins ($G\alpha_{i/o}$). Moreover, we found that human ferric bis-His Ngb acts as a guanine nucleotide dissociation inhibitor for $G\alpha_{i/o}$ that has been modified by oxidative stress. In addition, our data shows that Ngb inhibits the decrease in cAMP concentration that occurs under oxidative stress, leading to protection against cell death. Furthermore, by using a mutated Ngb protein that cannot form the bis-His conformation, we demonstrate that the oxidative stress-induced structural changes of human Ngb are essential for its neuroprotective activity.

Mammalian neuroglobin (Ngb)³ is an oxygen (O_2)-binding heme protein that has a classical globin fold and is widely expressed in the cerebral cortex, hippocampus, thalamus,

hypothalamus, cerebellum, and retina (1–3). Previous studies have shown that inhibiting Ngb expression with an antisense oligodeoxynucleotide decreases, while Ngb overexpression increases neuronal survival after oxidative stress, supporting the notion that mammalian Ngb protects neurons from hypoxic-ischemic insults (4–7). Mammalian Ngb has been reported to protect the brain from experimentally induced stroke *in vivo* (8, 9). Moreover, overexpression of Ngb in the hearts of transgenic mice reduced ischemic injury to myocardial cells, which contain vastly greater amounts of myoglobin (Mb) (8), suggesting that mammalian Ngb has a novel unique function, not shared by Mb, to protect against oxidative stress-induced cell death.

Mb is an intracellular globin that stores O_2 in muscle tissue and facilitates its diffusion from the periphery of the cell to the mitochondria. Although Ngb shares only 20–25% sequence identity with Mb, the key amino acid residues required for Mb function are conserved (1). The iron atom in the heme prosthetic group of each globin normally exists in either the ferrous (Fe^{2+}) or ferric (Fe^{3+}) redox state. In the absence of exogenous ligands, Mb is normally pentacoordinated in the ferrous form, leaving the sixth position available to bind exogenous ligands such as O_2 or carbon monoxide (CO), or hexacoordinated in the ferric state, with a water molecule coordinated to the ferric iron. In contrast, as shown in Fig. 1, both the ferric and ferrous forms of Ngb are hexacoordinated to endogenous protein ligands, namely proximal and distal histidine (His) residues, and O_2 or CO displaces the distal His residue of ferrous Ngb to produce ferrous O_2 - or CO-bound Ngb (10).

We previously found that the ferric form of human Ngb (HNgb) binds exclusively to the GDP-bound form of the α subunit of heterotrimeric G proteins ($G\alpha$) and competes with $G\beta\gamma$ for binding to $G\alpha$ (11, 12). Heterotrimeric G proteins consist of $G\alpha$ with GTPase activity and a $\beta\gamma$ dimer ($G\beta\gamma$) and belong to a family of proteins, whose signal transduction functions depend on the binding of guanine nucleotides (13–15). Ligand- or signal-activated G protein-coupled receptors (GPCRs) induce the release of GDP from $G\alpha$, allowing $G\alpha$ to bind to GTP. Binding of GTP to $G\alpha$ “turns on” the system and causes conformational changes that result in dissociation of the GTP-bound $G\alpha$ from both the receptor and $G\beta\gamma$. The GTP-bound $G\alpha$ and $G\beta\gamma$ can then regulate the activity of different effector molecules, such as

* This work was supported in part by the PRESTO program of Japan Science and Technology (JST) (to K. W.) and a Grant-in-Aid 23117704 for Scientific Research (to K. W.) from the Ministry of Education, Culture, Sports, Science and Technology of Japan.

¹ Supported by the JSPS Research Fellowships for Young Scientists. Present address: RIKEN Brain Science Institute, Wako, Saitama, Japan.

² To whom correspondence should be addressed: Department of Life Sciences, Graduate School of Arts and Sciences, The University of Tokyo, 3-8-1 Komaba, Meguro-ku, Tokyo 153-8902, Japan. Tel.: 81-3-5454-4392; Fax: 81-3-5454-4392; E-mail: wakasugi@bio.c.u-tokyo.ac.jp.

³ The abbreviations used are: Ngb, neuroglobin; Mb, myoglobin; GDI, guanine nucleotide dissociation inhibitor; HNgb, human Ngb; ZNgb, zebrafish Ngb; ROS, reactive oxygen species; M β CD, methyl- β -cyclodextrin; Rp-cAMPS, adenosine-3',5'-cyclic monophosphorothioate, Rp-isomer; Sp-cAMPS, adenosine-3',5'-cyclic monophosphorothioate, Sp-isomer; cAMP, adenosine-3',5'-cyclic monophosphate; TBE, trypan blue exclusion; MTS, 3-(4,5-dimethylthiazol-2-yl)-5-(3-carboxymethoxyphenyl)-2-(4-sulfophenyl)-2H-tetrazolium, inner salt; LDH, lactate dehydrogenase; IPTG, isopropyl- β -D-thiogalactopyranoside.

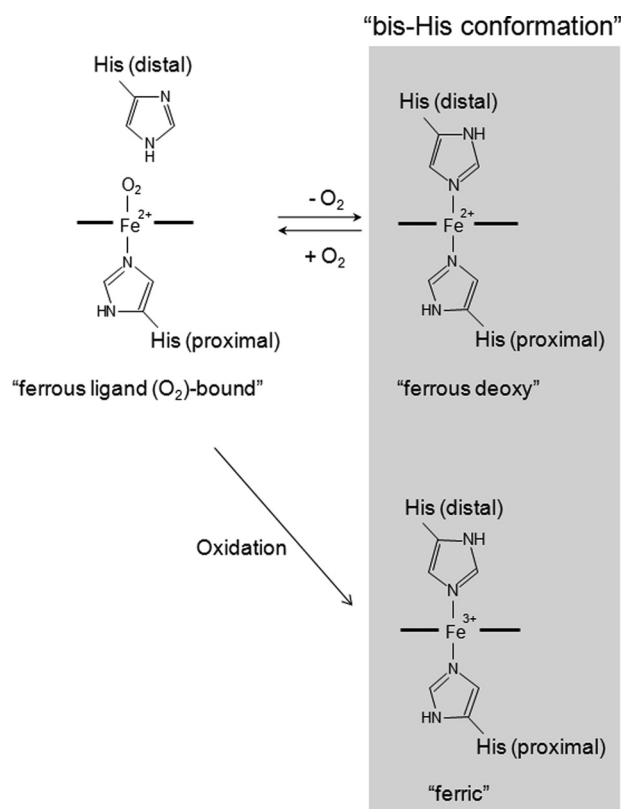


FIGURE 1. Schematic illustration of the heme environmental structures of ferrous ligand (O_2 or CO)-bound, ferrous deoxy, and ferric Ngb. The distal histidine residue of HNgb is His-64.

adenylyl cyclase, and ion channels. Signal transduction is “turned off” by the intrinsic GTPase activity of the $G\alpha$ protein, which hydrolyzes bound GTP to GDP, inducing the reassociation of GDP-bound $G\alpha$ to $G\beta\gamma$. $G\alpha$ proteins are grouped into four distinct families: $G\alpha_{i/o}$, $G\alpha_s$, $G\alpha_{q/11}$, and $G\alpha_{12/13}$ (14, 15). We previously showed that ferric HNgb binds exclusively to the GDP-bound form of $G\alpha_{i/o}$ and acts as a guanine nucleotide dissociation inhibitor (GDI) for $G\alpha_{i/o}$, whereas human Mb cannot interact with $G\alpha_{i/o}$ (12). In contrast, ferrous ligand-bound HNgb under normoxia does not interact with $G\alpha_{i/o}$ nor has GDI activity (11, 12). Together, these findings indicated that HNgb may be a novel oxidative stress-responsive sensor for signal transduction in the brain (12, 16).

Although Ngb was originally identified in mammalian species, it is also present in non-mammalian vertebrates (17, 18). Mammalian and fish Ngb proteins share about 50% amino acid sequence identity. Fish Ngb proteins are also hexacoordinated globins with similar oxygen-binding kinetics (18). Previously, we showed that zebrafish Ngb (ZNgb) has a cell membrane-penetrating activity (19–22), but does not exhibit GDI activity (23). To identify residues in HNgb that are crucial for its GDI activity, we previously generated HNgb mutants by focusing on those residues that differ between HNgb and ZNgb and on exposed residues with positive or negative charges on the protein surface (23). R47A, K102N, K119N, and D149A HNgb mutants, which retained GDI activity, protected PC12 cells against cell death caused by hypoxia/reoxygenation as did wild-type (WT) HNgb (7). In contrast, E53Q, R97Q, E118Q, and E151N HNgb mutants, which did not function as GDI proteins,

did not rescue cell death under oxidative stress conditions (7). These results clearly showed that the GDI activity of HNgb is tightly correlated with its neuroprotective activity.

Furthermore, we previously performed yeast two hybrid screening using HNgb as bait and identified flotillin-1 as a HNgb-binding protein (24). Flotillin-1 exists within lipid rafts, which are detergent-resistant, cholesterol- and sphingolipid-rich membrane domains that are involved in important cellular processes such as signal transduction and intracellular trafficking (25–29). Within the lipid rafts of the rat brain exist heterotrimeric G proteins (G_i , G_o , and G_s), Src family protein kinases, and some glycosylphosphatidylinositol (GPI)-anchored proteins (30–33). Flotillin-1 has been shown to recruit signaling proteins to lipid rafts that mediate the compartmentalization of crucial signal transduction pathways (27, 28). Because HNgb interacts with $G\alpha_{i/o}$, which also exists within lipid rafts, the association between HNgb and flotillin-1 may position it within lipid rafts containing heterotrimeric G proteins as a means of preventing neuronal death.

In the present study, we aimed to clarify the roles of lipid rafts in HNgb-mediated neuroprotection. Because $G\alpha_{i/o}$ proteins have been reported to be targets of reactive oxygen species (ROS) (34, 35), we investigated whether ferric HNgb interacts with the $G\alpha_{i/o}$ that is modified by ROS, thereby acting as a GDI for modified $G\alpha_{i/o}$. Moreover, we substituted the distal His residue with Val to create an HNgb mutant (H64V HNgb) that cannot form a bis-His conformation and investigated the significance of the structural changes of HNgb induced by oxidative stress.

EXPERIMENTAL PROCEDURES

Reagents—Rat myristoylated $G\alpha_{i1}$ was purchased from Calbiochem. The short splice variant of rat $G\alpha_s$ protein was obtained from Jena Bioscience (Jena, Germany). Horse heart Mb, and methyl- β -cyclodextrin (M β CD) were obtained from Sigma-Aldrich (St. Louis, MO). [8,5'- ^3H]GDP (20–50 Ci/mmol) was purchased from PerkinElmer Life Sciences (Boston, MA). Adenosine-3',5'-cyclic monophosphorothioate, Rp-isomer (Rp-cAMPS) and adenosine-3',5'-cyclic monophosphorothioate, Sp-isomer (Sp-cAMPS) were from Biolog (Bremen, Germany). Cholesterol was from Wako chemicals (Osaka, Japan).

Cell Culture—Rat pheochromocytoma PC12 cell line (RCB009) was obtained from the RIKEN Cell Bank (Ibaraki, Japan). PC12 cells were maintained in culture in Dulbecco's modified Eagle's medium (DMEM) containing glucose 4.5 g/liters, 10% (v/v) fetal bovine serum (FBS), 10% (v/v) heat-inactivated horse serum, 100 units/ml penicillin, 100 $\mu\text{g}/\text{ml}$ streptomycin, and 2 mM glutamine (all from Invitrogen (Carlsbad, CA)) in a humidified atmosphere containing 5% CO_2 at 37 $^\circ\text{C}$. The medium was changed twice weekly and the cultures were split at a 1:8 ratio once a week.

PC12 cells (CRL-1721.1) were obtained from the American Type Culture Collection (ATCC; Manassas, VA) and maintained in F-12 nutrient mixture (Ham's F-12), supplemented with 15% (v/v) horse serum, 2.5% (v/v) FBS, 100 units/ml penicillin, and 100 $\mu\text{g}/\text{ml}$ streptomycin (all from Invitrogen) in a humidified atmosphere containing 5% CO_2 at 37 $^\circ\text{C}$. The

Neuroprotective Mechanism of Human Neuroglobin

medium was changed every 3 days, and the cultures were split at a 1:8 ratio once a week.

SH-SY5Y human neuroblastoma cells (CRL-2266) were obtained from ATCC and maintained in a 1:1 mixture of DMEM and Ham's F-12 containing 2.5 mM glutamine, supplemented with 10% (v/v) FBS, 100 units/ml penicillin, and 100 μ g/ml streptomycin (all from Invitrogen) in a humidified atmosphere containing 5% CO₂ at 37 °C. The medium was changed every 4 days, and the cultures were split at a 1:20 ratio once a week. Cultured cells were induced to differentiate into a neuronal phenotype by treatment with 10 μ M retinoic acid (Sigma-Aldrich) over a period of 6 days (media were exchanged every 3 days during sub-culture). Differentiation was verified by monitoring macroscopic changes to the cells.

Detergent Solubilization and Sucrose Density Gradient Fractionation—HNgb cDNA was cloned into the eukaryotic expression vector pcDNA3.1 (Invitrogen). The construct was confirmed by DNA sequencing (FASMAC Co., Ltd., DNA sequencing services). The PC12 cells (CRL-1721.1) were grown on 100-mm dishes until 70–80% confluence. The pcDNA3.1-HNgb expression vector was transfected using LipofectamineTM 2000 (Invitrogen) according to the manufacturer's instructions. After 24 h of transfection, the cells were incubated for 3 h in the absence or presence of 200 μ M hydrogen peroxide. The cells were washed twice with ice-cold buffer A (25 mM Tris-HCl, 150 mM NaCl, 5 mM EDTA, pH 7.5) and then resuspended in 2 ml of ice-cold carbon monoxide (CO)-saturated buffer A containing 1% Brij-58 [polyoxyethylene(20)cetyl ether], 0.4% (v/v) PMSF and complete, EDTA-free; protease inhibitor mixture (Roche Diagnostics, Mannheim, Germany), and incubated at 4 °C for 20 min. The cells were homogenized with 10 strokes of a Dounce homogenizer, and 1.5 ml of the homogenate was added to an equal volume of 80% (w/v) sucrose in buffer A. The solubilized cells (in 40% sucrose) were overlaid successively with 6 ml of 30% (w/v) sucrose and 4 ml of 5% (w/v) sucrose in buffer A. After centrifugation at 18,000 rpm in a Beckman SW41 Ti rotor for 18 h at 4 °C, 12 fractions of 1 ml each were collected from the top. Fractions 1–9 were concentrated with ice-cold trichloroacetic acid. The 12 gradient fractions were analyzed by immunoblotting with rabbit anti-HNgb (FL-151) polyclonal antibody (Santa Cruz Biotechnology, Santa Cruz, CA), or rabbit anti-flotillin-1 (H-104) polyclonal antibody (Santa Cruz Biotechnology). Can Get Signal[®] immunoreaction enhancer solution (Toyobo, Tokyo, Japan) was used in the antibody dilution buffer to reduce the background level for the Western blot analyses.

Lipid Raft Disassembly by M β CD—Differentiated SH-SY5Y cells were plated on poly-D-lysine-coated 96-well tissue culture plates at a density of 5.0×10^5 cells/ml for 24 h. The pcDNA3.1-HNgb expression vector or control vector (pcDNA3.1 empty vector) was transfected by using LipofectamineTM 2000 (Invitrogen) as directed by the manufacturer. After 24 h of transfection, the cells were incubated in serum-free media containing 1.4 mM M β CD for 30 min at 37 °C. In a separate set of experiments, cholesterol was added back to cholesterol-depleted cell cultures in order to reconstitute the disassembled rafts. In brief, repletion with cholesterol was accomplished by incubating cells in the presence of a 0.18 mM cholesterol/1.4 mM M β CD mixture for 1 h at 37 °C. A stock

solution of 1.0 mM cholesterol and 7.6 mM M β CD was prepared by vortexing at 40 °C in 1 ml of 7.6 mM M β CD with 20 μ l/liter of cholesterol (20 mg/ml in ethanol solution). The culture medium was replaced with fresh growth medium, and the cells were then treated with 100 μ M hydrogen peroxide for 24 h at 37 °C.

Cell Viability Assays—Cell viability was measured by trypan blue exclusion (TBE) assays. Trypan blue was added to the cultured cells, and the percentage of blue-stained cells was calculated after counting at least 1000 cells via phase contrast microscopy. Cell viability was also measured with CellTiter 96[®] Aqueous One Solution Cell Proliferation Assay Reagent (Promega, Madison, WI), containing [3-(4,5-dimethylthiazol-2-yl)-5-(3-carboxymethoxyphenyl)-2-(4-sulfophenyl)-2H-tetrazolium, inner salt; MTS]. The cultured cells were incubated with the MTS reagent at 37 °C for 4 h in a humidified, 5% CO₂ atmosphere. The amount of colored formazan dye formed was then quantified by measuring absorbance at 490 nm with a Beckman Coulter DTX880 plate reader (Beckman Coulter, Fullerton, CA). Cell viability was also assessed by lactate dehydrogenase (LDH) assays using CytoTox 96[®] Non-Radioactive Cytotoxicity Assay kit (Promega) according to the manufacturer's directions.

Preparation and Purification of Glutathione S-Transferase (GST) and a Fusion Protein of GST and Ngb—HNgb or ZNgb cDNA was cloned into the pGEX-4T-1 vector (GE Healthcare Biosciences, Piscataway, NJ) to produce the fusion protein GST-Ngb (24). Overexpression of GST-Ngb and GST alone (as a control) was induced in the *Escherichia coli* strain BL21 (DE3) (Novagen, Madison, WI) by treatment with isopropyl- β -D-thiogalactopyranoside (IPTG) for 4 h. Both GST-Ngb and GST were purified by using glutathione-Sepharose 4B beads (GE Healthcare Biosciences) according to the manufacturer's instructions. The binding buffer contained 1 mM dithiothreitol (DTT). The purified proteins were then loaded onto a HiTrap Q HP cartridge (GE Healthcare Biosciences) equilibrated with 50 mM Tris-HCl, pH 8.0, and eluted with a linear NaCl gradient from 0 to 0.7 M.

Preparation and Purification of Human Truncated Flotillin-1 (a.a. 137–427)—Human truncated flotillin-1 was expressed in *Escherichia coli* and purified as described previously (24).

GST Pull-down Assays of Truncated Flotillin-1—Human truncated flotillin-1, solubilized in buffer (8 M urea, 100 mM sodium phosphate buffer, and 10 mM Tris-HCl, pH 4.5), was diluted 16 times with buffer B (50 mM Tris-HCl, 150 mM NaCl, 2 mM EDTA, 1% Nonidet P-40, pH 7.4 or pH 8.0) containing EDTA-free complete protease inhibitor mixture (Roche Diagnostics). The diluted sample was then concentrated and incubated with either GST alone or GST-Ngb immobilized on glutathione-Sepharose 4B beads (GE Healthcare Biosciences) for 1 h at 4 °C. The beads were washed extensively three times with buffer B. The samples were then resuspended in Laemmli sample buffer, heated for 5 min at 95 °C, and separated by 12.0% SDS/PAGE. For Western blot analyses, the proteins were transferred onto Hybond-P PVDF membranes (GE Healthcare Biosciences), which were then blocked with phosphate-buffered saline (PBS) and 5% skim milk (Wako chemicals) and incubated

with rabbit anti-flotillin-1 (H-104) polyclonal antibody (Santa Cruz Biotechnology). The membranes were washed and then incubated with an HRP-linked F(ab')₂ fragment of donkey anti-rabbit IgG (GE Healthcare Biosciences).

GST Pull-down Assays using a Rat Brain Extract—Freshly excised SD rat brains purchased from Japan SLC (Shizuoka, Japan) were homogenized on ice in Tris-buffered saline buffer (50 mM Tris-HCl, 100 mM NaCl, 1 mM DTT, and 1 mM EDTA, pH 8.0) containing 1% n-octyl- β -glucoside and protease inhibitor mixture. The homogenates were incubated on ice, and insoluble fractions were removed by centrifugation. The supernatants were used in the GST pull-down assays. The experimental conditions of the GST pull-down assays have been described above for recombinant truncated flotillin-1.

Construction, Expression, and Purification of Recombinant Human $G\alpha_{i1}$ Protein—The DNA fragment containing the human $G\alpha_{i1}$ subunit (residues 1–354) was amplified by PCR and cloned into the pET151/D-TOPO[®] vector (Invitrogen) to be expressed as human wild-type $G\alpha_{i1}$ protein fused to a TEV protease recognition site directly after an N-terminal tag of six histidine residues (His-tag). The construct was confirmed by DNA sequencing (FASMAC Co., Ltd., DNA sequencing services). The resulting $G\alpha_{i1}$ was expressed in the *Escherichia coli* strain BL21 (DE3) by induction with 30 μ M IPTG for 18 h at 25 °C. Cells were extracted in buffer C (50 mM Tris-HCl (pH 8.0), 300 mM NaCl, 10 mM imidazole, 20 mM β -mercaptoethanol, 0.4% (v/v) phenylmethylsulfonylfluoride (PMSF)) supplemented with complete, EDTA-free; protease inhibitor mixture (Roche Diagnostics). After centrifuging at 10,000 rpm for 30 min at 4 °C, the supernatant including human $G\alpha_{i1}$ protein with His-tag was applied to a nickel affinity column (His-Bind[®] resin; Novagen) equilibrated with buffer C. The column was washed with 50 mM Tris-HCl (pH 8.0), 300 mM NaCl, 20 mM imidazole, 20 mM β -mercaptoethanol and 0.4% (v/v) PMSF. $G\alpha_{i1}$ was then eluted with 50 mM Tris-HCl (pH 8.0), 300 mM NaCl, 250 mM imidazole, 20 mM β -mercaptoethanol, and 0.4% (v/v) PMSF. The buffer was immediately replaced with 50 mM Tris-HCl (pH 8.0), 150 mM NaCl, 50 μ M GDP, 20 mM β -mercaptoethanol and 0.4% (v/v) PMSF. To eliminate the N-terminal His-tag from $G\alpha_{i1}$, the sample was incubated for 24 h at 4 °C with His-tagged TEV protease (MoBiTec GmbH, Göttingen, Germany) added in a ratio of 1:200 (w/w). The sample was then loaded onto a His-Bind[®] column equilibrated with buffer C to separate the cleaved $G\alpha_{i1}$ from the cleaved His-tag, any uncleaved protein, and His-tagged TEV protease. The purified $G\alpha_{i1}$ (flow-through fraction) was concentrated in 50 mM HEPES (pH 8.0), 1 mM EDTA, 2 mM DTT, and 200 μ M GDP and stored at –80 °C.

GST Pull-down Assays using $G\alpha_{i1}$ or $G\alpha_s$ — $G\alpha_{i1}$ or $G\alpha_s$ was incubated with either GST alone or GST-Ngb immobilized on glutathione-Sepharose 4B beads (GE Healthcare Biosciences) in HEPES buffer (10 mM HEPES, 150 mM NaCl, 10 mM MgCl₂, 10 μ M GDP, 0.1% Tween 20, pH 7.4) in the absence or presence of 10 mM NaF and 30 μ M AlCl₃ for 1 h at 4 °C. The beads were washed extensively three times with the buffer, and the samples were then resuspended in Laemmli sample buffer, heated for 5 min at 95 °C, and separated by 12.0% SDS/PAGE. For Western blot analyses, the proteins were transferred onto Hybond-P

PVDF membranes (GE Healthcare Biosciences), which were then blocked with PBS and 5% skim milk (Wako chemicals) and incubated with mouse anti- $G\alpha_{i1}$ (Ab-3; clone R4.5) monoclonal antibody (Thermo Fisher Scientific, Fremont, CA) or mouse anti- $G\alpha_s$ (12) monoclonal antibody (Santa Cruz Biotechnology). After washing, the membranes were incubated with an HRP-linked whole antibody of sheep anti-mouse IgG (GE Healthcare Biosciences).

Treatment of $G\alpha_{i1}$ with ROS—For preparation of ROS-treated $G\alpha_{i1}$, 100 μ M $G\alpha_{i1}$ was incubated with 1 mM hydrogen peroxide and 1 mM FeSO₄ for 10 min at 25 °C. Next, the protein was purified by Sephadex G25 column chromatography. ROS-treated $G\alpha_{i1}$ was stored in 50 mM HEPES (pH 8.0), 1 mM EDTA, and 200 μ M GDP at –80 °C.

UV-Visible Spectra—Electronic absorption spectra of purified proteins in PBS (pH 7.4) were recorded with a UV-visible spectrophotometer (UV-2450; Shimadzu, Kyoto, Japan) at ambient temperature (~20 °C).

Preparation of Ngb Proteins—Plasmids for HNgb or ZNgb were prepared as described previously (12, 23). A Quik-Change[™] site-directed mutagenesis system (Stratagene, La Jolla, CA) was used to introduce substitutions at specific sites according to the manufacturer's instructions. The constructs were confirmed by DNA sequencing (FASMAC Co., Ltd., DNA sequencing services, Atsugi, Japan). Overexpression of each Ngb was induced in the *E. coli* strain BL 21 (DE 3) by treatment with IPTG, and each Ngb protein was purified as previously described (7, 20, 23). Briefly, soluble cell extracts were loaded onto DEAE Sepharose anion-exchange columns equilibrated with buffer D (20 mM Tris-HCl, pH 8.0). Ngb proteins were eluted from the columns with buffer D containing 75 mM NaCl and further purified by passage through Sephacryl S-200 HR gel filtration columns. Ngb proteins were then applied to a HiTrap Q HP column (GE Healthcare Bio-Sciences) and eluted with a 0–500 mM linear NaCl gradient in buffer D. Purified Ngb was dialyzed overnight against PBS. Endotoxin was removed from the protein solutions by phase separation using Triton X-114 (Sigma-Aldrich) (36, 37). Trace amounts of Triton X-114 were removed by passage through Sephadex G25 gel (GE Healthcare Bio-Sciences) equilibrated with PBS. The protein concentration of human ferric Ngb was determined spectrophotometrically using an extinction coefficient of 122 mm⁻¹ cm⁻¹ at the Soret peak.

Purified H64V HNgb was in the ferrous O₂-bound form. Ferric H64V HNgb was obtained by treating the protein with a 20% excess of K₃Fe(CN)₆ and quickly passing the resulting solution over a Sephadex G25 gel filtration column equilibrated with PBS (pH 7.4).

[³H]GDP Dissociation Assays— $G\alpha_{i1}$ complexed with [³H]GDP (0.3 μ M) was prepared by incubating 0.3 μ M $G\alpha_{i1}$ with 2 μ M [³H]GDP in buffer E (20 mM Tris-HCl, 100 mM NaCl and 10 mM MgSO₄ at pH 8.0) with or without 2 mM DTT for 1.5 h at 25 °C. Excess unlabeled GTP (2 mM) was added to monitor dissociation of [³H]GDP from $G\alpha_{i1}$ in the absence or presence of Ngb (10 μ M). Aliquots were withdrawn at 0, 5, and 10 min and were passed through nitrocellulose filters (0.45 μ m) (Advantec Toyo). The filters were then washed three times with 1 ml of

Neuroprotective Mechanism of Human Neuroglobin

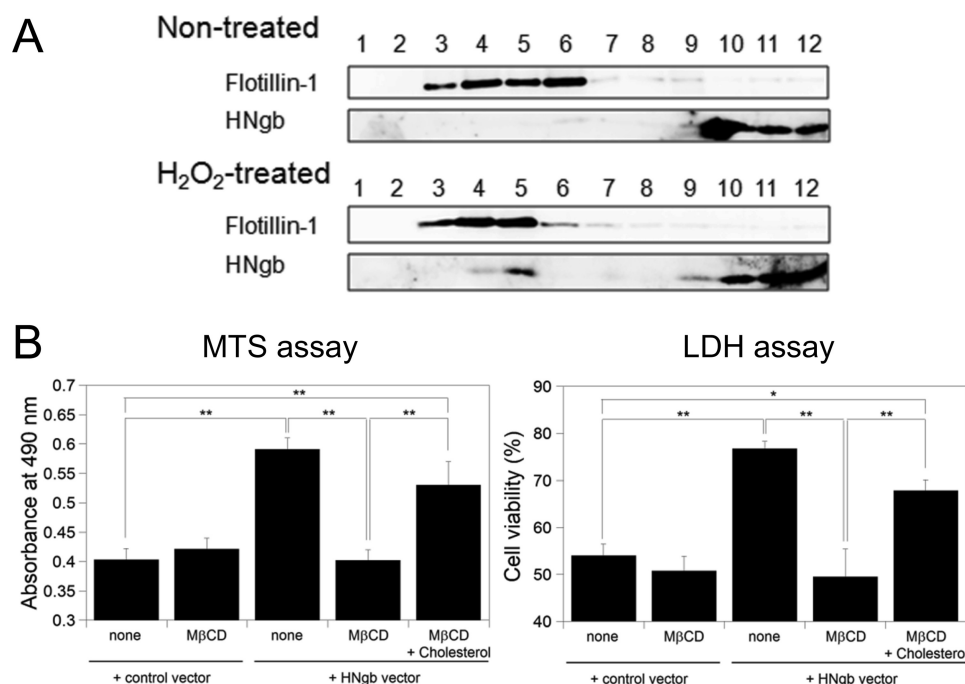


FIGURE 2. Lipid rafts are crucial for neuroprotection by HNgB. A, NgB increases in lipid rafts in PC12 cells during oxidative stress. PC12 cells were incubated in the absence or presence of hydrogen peroxide. Lipid rafts were isolated by Brij58 treatment and sucrose gradient fractionation. NgB and flotillin-1 were separated by 15.0% and 12.0% SDS-PAGE, and detected with anti-NgB and anti-flotillin-1 antibody, respectively. B, addition of MβCD attenuated neuroprotective activity by HNgB, whereas reconstruction of lipid raft domains by addition of cholesterol restored it. Differentiated SH-SY5Y cells were treated with hydrogen peroxide, and cell viability was assessed by MTS and LDH assays. Each graph represents data from three independent experiments, each carried out in triplicate. All data are expressed as means ± S.E. of means (S.E.). *, $p < 0.05$, **, $p < 0.01$.

ice-cold buffer E and were counted in a liquid scintillation counter (LS6500; Beckman Coulter).

Treatment of SH-SY5Y Cells with cAMP Analog or Antagonist and Hydrogen Peroxide—Differentiated SH-SY5Y cells were plated on poly-D-lysine coated 96-well plates at a density of 5.0×10^5 cells/ml for 24 h. The pcDNA3.1-HNgB expression vector or control vector (pcDNA3.1 empty vector) was transfected by using LipofectamineTM 2000 (Invitrogen) according to the manufacturer's instructions. After 24 h of transfection, cells were treated with Sp-cAMPS or Rp-cAMPS at a concentration of 300 μ M for 1 h. The hydrogen peroxide was then added at 100 μ M, and cells were incubated for 24 h.

cAMP Immunoassay—Differentiated SH-SY5Y cells were seeded at 5.0×10^5 /ml in 12-well cell culture plates the day before experiments. The control vector (pcDNA3.1 empty vector) or pcDNA3.1-HNgB expression vector was transfected by using LipofectamineTM 2000 (Invitrogen) according to the manufacturer's instructions. After 24 h of transfection, the cells were treated with 100 μ M hydrogen peroxide for 24 h at 37 °C. Then, the concentrations of intracellular cAMP were determined using cAMP BiotrakTM competitive enzymeimmunoassay system (GE Healthcare Biosciences) according to the manufacturer's instructions.

Protein Transduction by Chariot—Protein transduction was performed by using ChariotTM (Active Motif, Carlsbad, CA) as described previously (7, 20). Each purified globin protein (3 μ g per well) was incubated in the presence of diluted Chariot for 30 min at room temperature. Next, the mixture was added to cells that had been washed in DMEM without serum. DMEM without serum was added and the cells were incubated at 37 °C for

1 h; FBS was then added to a final concentration of 2%. The cells were incubated at 37 °C for another 2 h to allow NgB internalization.

Protein transduction was confirmed by Western blot analyses using rabbit anti-HNgB (FL-151) polyclonal antibody (Santa Cruz Biotechnology), mouse anti- β -actin monoclonal antibody (Sigma-Aldrich), or rabbit anti-Mb polyclonal antibody (Spring Bioscience, Pleasanton, CA).

Hypoxia/Reoxygenation—PC12 cells (RCB009) were plated on a poly-D-lysine-coated 96-well tissue culture plate at a density of 1.0×10^5 cells/ml in DMEM containing 2.0 g/liter glucose, 2% (v/v) FBS, and 2 mM glutamine for 24 h. Each NgB was transduced with or without ChariotTM. Hypoxia was induced in a multigas incubator (Astec, Fukuoka, Japan; set to 1% O₂, with 5% CO₂ and 94% N₂) at 37 °C for 24 h. After hypoxia, the culture medium was replaced with fresh DMEM containing 2.0 g/L glucose, 2% (v/v) FBS, and 2 mM glutamine, and the cells were incubated at 37 °C for 24 h under normoxia (95% air/5% CO₂).

Statistics—Data were analyzed by one-way ANOVA followed by Tukey-Kramer post hoc tests.

RESULTS

NgB Levels Increase in Lipid Rafts under Oxidative Stress, and Lipid Rafts Are Essential for the Neuroprotective Activity of HNgB—First, we examined whether oxidative stress affects the intracellular localization of NgB in PC12 cells. Lipid rafts were isolated conventionally by treatment with Brij-58. The 12 gradient fractions were then analyzed by immunoblotting with anti-flotillin-1 or anti-NgB antibody. Flotillin-1, a marker for lipid rafts, was found intensively in fractions 3–6 (Fig. 2A), indi-

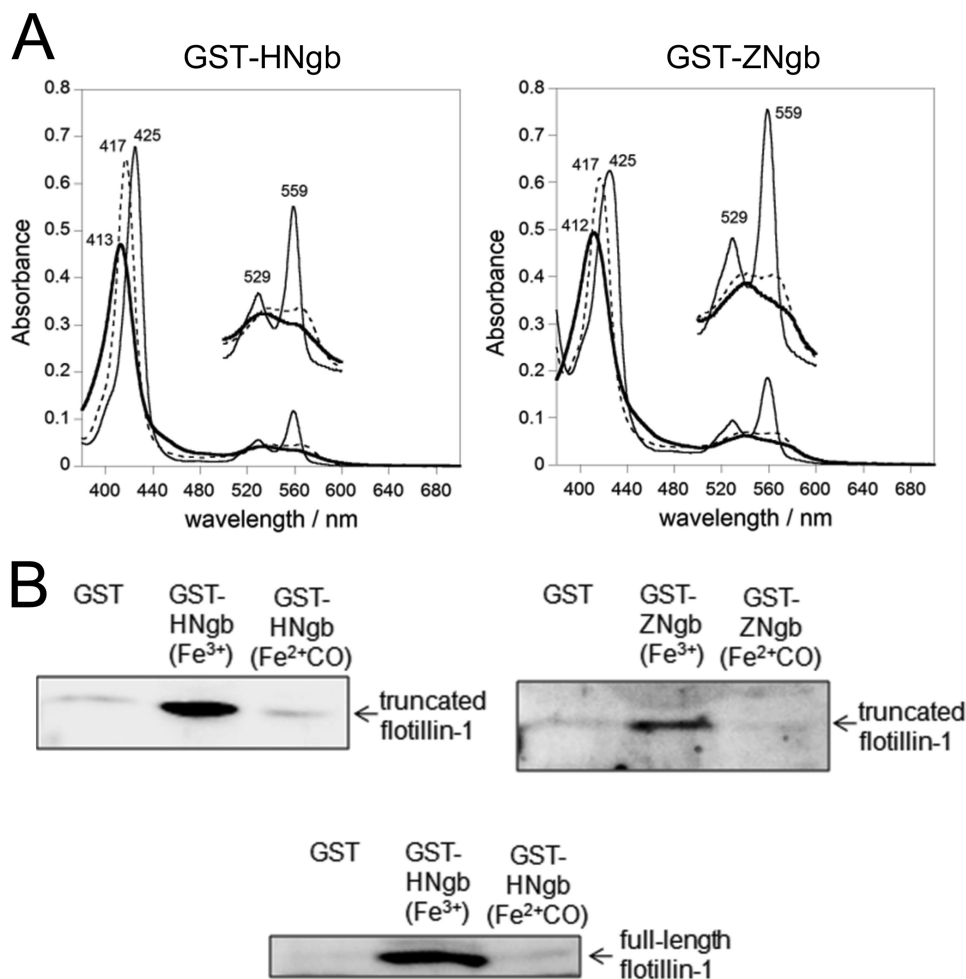


FIGURE 3. Structural and flotillin-1-binding properties of GST-fused HNgb or ZNgb. *A*, electronic absorption spectra of the ferric (**bold line**), ferrous deoxy (**fine line**), and ferrous-CO (**dotted line**) forms of GST-fused HNgb or GST-fused ZNgb. The concentration of each recombinant protein was $\sim 5 \mu\text{M}$ on the basis of heme content. The Q bands from 500 to 600 nm are enlarged by a factor of 3 on the perpendicular axis. *B*, GST pull-down assays with Ngb and flotillin-1. Truncated or full-length flotillin-1 was incubated with GST-HNgb, GST-ZNgb, or GST in buffer (pH 8.0), washed, and analyzed by Western blotting with rabbit anti-flotillin-1 polyclonal antibody.

cating that lipid rafts float into these fractions during centrifugation. Ngb was detected not only in fractions 10–12 at the bottom of the gradient but also in fraction 5 of lipid rafts under hydrogen peroxide-induced oxidative stress. Thus, these results indicate that part of Ngb is recruited to lipid rafts in PC12 cells only during oxidative stress.

Because raft domains are enriched in cholesterol, a compound that interacts with and sequesters cholesterol may be a useful tool for investigating the structural and functional significance of plasma membrane compartments. M β CD, known as a lipid raft-disrupting agent, extracts cholesterol from the plasma membrane (29, 38). To investigate the role of lipid rafts in the signaling process, SH-SY5Y cells were pretreated with M β CD to ablate raft structures and were exposed to hydrogen peroxide. Addition of M β CD attenuated the neuroprotective activity of HNgb (Fig. 2*B*) as shown by cell viability assays. To restore cholesterol-rich raft domains, cholesterol-depleted cell cultures were incubated with cholesterol-loaded M β CD. After raft constitution, cells were exposed to hydrogen peroxide. Reconstitution of the lipid raft domains restored the neuroprotective activity of HNgb (Fig. 2*B*). Taken together, these findings suggest that plasma membrane compartments rich in cholesterol

participate in HNgb-mediated signal transduction pathways during oxidative stress.

Ferric, but Not Ferrous Ligand-bound, HNgb Binds to Flotillin-1—In the present study, we carried out GST pull-down assays in which GST-fused HNgb or ZNgb was used to characterize the interaction of Ngb and proteins *in vitro*. Because ferrous O₂-bound Ngb is unstable and is converted into ferric Ngb very rapidly due to autoxidation (10), stable ferrous carbon monoxide (CO)-bound Ngb was used as a model of ferrous O₂-bound Ngb in the following experiments. As shown in Fig. 3*A*, the UV-visible spectra of GST-Ngb indicated that both GST-HNgb and GST-ZNgb form a ferric, ferrous deoxy, or ferrous ligand-bound state, as does untagged Ngb (39).

Previously, we showed that ferric HNgb, which is generated spontaneously as a result of rapid autoxidation, interacts with a truncated human flotillin-1 protein (a.a. 137–427) and with WT rat flotillin-1 (24). In the present study, we investigated whether ZNgb or ferrous ligand-bound HNgb interacts with flotillin-1. As shown in Fig. 3*B*, the ferric form, but not the ferrous CO-bound form of HNgb or ZNgb interacts with truncated human flotillin-1 (Fig. 3*B*). Moreover, we demonstrated

Neuroprotective Mechanism of Human Neuroglobin

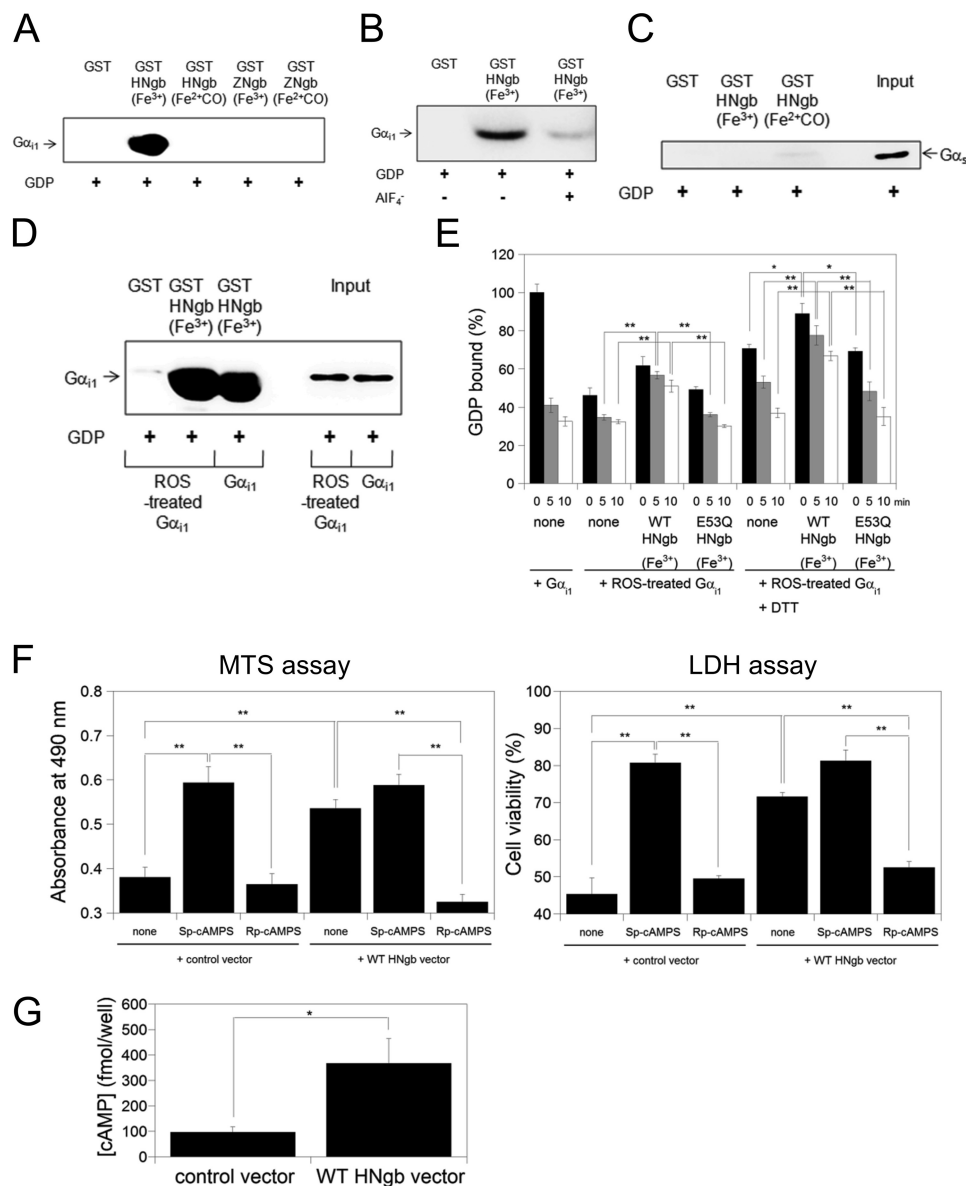


FIGURE 4. Structural and $G\alpha_{11}$ -binding properties of HNgb or ZNgb. *A*, GST pull-down assays with Ngb and rat myristoylated GDP-bound $G\alpha_{11}$. Western blot analyses were performed with anti- $G\alpha_{11}$ mouse monoclonal antibody. *B*, comparison of HNgb binding between different forms of recombinant human $G\alpha_{11}$. GDP-bound $G\alpha_{11}$ in the absence or presence of AIF_4^- was incubated with GST-HNgb or GST. *C*, GST pull-down assays with HNgb and $G\alpha_s$. GDP-bound $G\alpha_s$ was incubated with GST-HNgb or GST, washed, and analyzed by Western blotting with anti- $G\alpha_s$ antibody. *D*, GST pull-down assays with HNgb and ROS-treated $G\alpha_{11}$. GST-HNgb or GST was incubated with untreated or ROS-treated human $G\alpha_{11}$. The same concentration and volume of untreated and ROS-treated human $G\alpha_{11}$ were used. *E*, effects of HNgb on dissociation of GDP from untreated or ROS-treated $G\alpha_{11}$. The amount of [³H]GDP bound to untreated $G\alpha_{11}$ in the absence of HNgb at 0 min was defined as 100%. Data are expressed as means \pm S.E. from four independent experiments. *, $p < 0.05$, **, $p < 0.01$. *F*, protection by HNgb is mediated by cAMP. Differentiated SH-SY5Y cells were pretreated with Sp-cAMPS or Rp-cAMPS, and then incubated with hydrogen peroxide. Cell viability was measured by MTS and LDH assays. Each graph represents data from three independent experiments each carried out in triplicate. Data are expressed as means \pm S.E. **, $p < 0.01$. *G*, WT HNgb increases intracellular cAMP concentration under oxidative stress. Differentiated SH-SY5Y cells were treated with hydrogen peroxide, and intracellular cAMP concentrations were determined by cAMP enzyme immunoassay kit. Data are expressed as means \pm S.E. from five experiments. *, $p < 0.05$.

that ferric, but not ferrous CO-bound HNgb binds to full-length WT flotillin-1 (Fig. 3B).

Ferric HNgb Acts as a GDI for $G\alpha_{i/o}$ Modified by ROS and Inhibits the Oxidative Stress-mediated Decrease in cAMP to Protect against Cell Death—Using surface plasmon resonance, we previously showed that ferric HNgb binds exclusively to GDP-bound $G\alpha_{i/o}$, whereas ferrous CO-bound HNgb does not interact with $G\alpha_{i/o}$ (12). Moreover, GST pull-down assays using GST-fused HNgb have demonstrated that GST-ferric, but not GST-ferrous CO-bound HNgb interacts with $G\alpha_i$ (11, 16).

These data are consistent with those obtained by surface plasmon resonance of untagged Ngb (12), suggesting that the GST tag has no effect on protein-protein interactions between HNgb and $G\alpha_i$.

In the present study, GST-HNgb, GST-ZNgb, or GST was incubated with rat myristoylated $G\alpha_{11}$, and Western blot analyses were performed by using antibody against $G\alpha_{11}$. As shown in Fig. 4A, ferric bis-His HNgb, but not ferrous CO-bound HNgb or ferric or ferrous CO-bound ZNgb, bound to the GDP-bound form of rat myristoylated $G\alpha_{11}$. Moreover, ferric HNgb

bound to the GDP-bound form of nonmyristoylated $G\alpha_{11}$ expressed in *E. coli* (Fig. 4B). Aluminum tetrafluoride (AlF_4^-) can interact with $G\alpha_{11}$ -bound GDP and mimic GTP, thereby activating $G\alpha_{11}$ (14). In the presence of GDP and AlF_4^- , ferric HNgB did not bind to activated $G\alpha_{11}$ (Fig. 4B). Therefore, ferric HNgB clearly interacts with the inactive (GDP-bound) form of $G\alpha_{11}$. Moreover, we clarified that HNgB does not bind to $G\alpha_s$ (Fig. 4C).

$G\alpha_{i/o}$ proteins are targets of ROS, which directly activate $G\alpha_{i/o}$ without receptor activation by modification of specific cysteine residues that exist only in $G\alpha_{i/o}$ but not in other $G\alpha$ families, leading to the selective activation of $G\alpha_{i/o}$ under conditions of oxidative stress (34, 35). ROS, such as hydroxyl radical, were generated in the presence of hydrogen peroxide and Fe^{2+} . GST pull-down assays showed that WT HNgB interacts comparably with ROS-modified and non-modified $G\alpha_{11}$ (Fig. 4D). Two cysteine residues of $G\alpha_{i/o}$ have been reported to be oxidized by ROS, leading to activation of $G\alpha_{i/o}$ and dissociation into $G\alpha_{i/o}$ and $G\beta\gamma$ (35). Fig. 4E shows that modification of $G\alpha_{11}$ by ROS decreased the percentage of GDP-bound $G\alpha_{11}$ at 0 min as compared with non-modified $G\alpha_{11}$, suggesting that modified $G\alpha_{11}$ has decreased affinity for GDP. This is consistent with previous data that $G\alpha_{i/o}$ mutated on a Cys residue that is modified by ROS showed decreased affinity for GDP under normal conditions (40). As shown in Fig. 4E, WT HNgB functioned as a GDI for modified $G\alpha_{11}$, whereas the E53Q HNgB mutant did not. Treatment with DTT significantly increased the percentage of GDP-bound form of $G\alpha_{11}$ (Fig. 4E), suggesting that cysteine residues of $G\alpha_{11}$ are modified by ROS.

Next, we considered whether HNgB may protect neuronal cells by increasing intracellular levels of cAMP. Sp-cAMPS and Rp-cAMPS are an activator and an inhibitor, respectively, of cAMP-dependent protein kinases. Incubation of cells with the stable cAMP analog Sp-cAMPS led to protection during oxidative stress induced by hydrogen peroxide (Fig. 4F). In contrast, the cAMP antagonist Rp-cAMPS did not rescue cell death. To verify this relationship between protection by HNgB and cAMP levels, we inhibited cAMP signaling by adding Rp-cAMPS prior to hydrogen peroxide treatment. This led to a significant reduction in HNgB-mediated protection (Fig. 4F). Next, we measured the intracellular concentration of cAMP in SH-SY5Y cells transfected with the control vector or WT HNgB expression vector under hydrogen peroxide-induced oxidative stress. As shown in Fig. 4G, WT HNgB significantly increased the amount of intracellular cAMP under oxidative stress. Taken together, these data suggest that neuroprotective activity by HNgB is correlated with increasing cAMP concentration.

A Structural Change in HNgB Induced by Oxidative Stress Is Crucial for Its Neuroprotective Activity—To investigate the effects of structural changes in HNgB on its neuroprotective activity, we prepared an H64V HNgB mutant, in which the distal His residue was substituted with Val, as a model of HNgB that cannot form a bis-His conformation. The UV-visible spectra recorded immediately after purification of H64V HNgB showed features typical of ferrous O_2 -bound globins. Ferrous O_2 -bound H64V HNgB was converted to its ferric form by the addition of ferricyanide. The Soret peak of ferric H64V HNgB was 406 nm, corresponding to previous observations (41, 42).

These data confirm that ferric H64V HNgB forms a mono-His conformation as does ferric Mb.

As shown in Fig. 5A, the GST-fused H64V HNgB mutant did not interact with human $G\alpha_{11}$ or flotillin-1, suggesting that H64V HNgB can be used as a model of ferrous ligand-bound HNgB, which does not form the bis-His conformation. To examine the effect of H64V mutation of HNgB on the release of GDP from $G\alpha_{11}$, we measured the rates of GDP dissociation in the absence or presence of HNgB. In the presence of an excess amount of unlabeled GTP, [3H]GDP release from [3H]GDP-bound $G\alpha_{11}$ was inhibited by ferric WT HNgB (Fig. 5B). In contrast, ferric H64V HNgB did not act as a GDI for $G\alpha_{11}$ (Fig. 5B). Next, we tested whether H64V HNgB can protect cells against hypoxia/reoxygenation, which induces oxidative stress by generating ROS (43). Protein transduction was achieved by using the protein delivery reagent Chariot, which can efficiently deliver a variety of proteins into several cell lines in a fully biologically active form (7, 20, 44, 45), and was confirmed by Western blot analyses (Fig. 5C). MTS assays showed that cell survival was significantly enhanced by the transduction of WT HNgB into PC12 cells (Fig. 5D). TBE assays also showed that protein transduction of WT HNgB with Chariot resulted in a significant increase in cell viability (Fig. 5D). These results suggest that WT HNgB is effective in rescuing PC12 cell death induced by hypoxia/reoxygenation. By contrast, H64V HNgB, which cannot form the bis-His conformation, did not significantly rescue cell death during oxidative stress (Fig. 5D). These results indicate that oxidative stress-induced structural change in HNgB is crucial for its neuroprotective activity. As shown in Fig. 5D, Mb, which does not interact with $G\alpha_{11}$ (12), did not protect PC12 cells against cell death caused by hypoxia/reoxygenation and did not induce PC12 cell death, similar to the PBS control.

DISCUSSION

In the present study, we found that NgB exists in lipid rafts only during oxidative stress. In addition, our data shows that addition of a lipid raft disruptor, M β CD, attenuates the neuroprotective activity of HNgB, whereas reconstruction of lipid raft domains restores it, suggesting that lipid rafts are crucial for NgB-mediated neuroprotection. Because HNgB binds to flotillin-1, a lipid raft microdomain-associated protein (24), and $G\alpha_{i/o}$ also exists in lipid rafts (30–33), flotillin-1 recruits HNgB to lipid rafts, where HNgB then binds to $G\alpha_{i/o}$ and acts as a GDI for $G\alpha_{i/o}$, as a means of preventing neuronal death (Fig. 6A).

We clarified that ferric bis-His, but not ferrous ligand-bound HNgB interacts with both flotillin-1 and $G\alpha_{11}$. Moreover, we showed that the H64V HNgB mutant, which cannot form a bis-His conformation, did not interact with $G\alpha_{11}$ or flotillin-1. Molecular dynamics simulations of mouse ferrous deoxy and CO-bound NgB have documented that alteration of the His configuration upon CO binding changes the dynamic behavior of the CD corner, which comprises α -helices C and D and the CD loop (46). Glu-53, which we identified as crucial for the HNgB- $G\alpha_{11}$ interaction (23), is located in the CD corner of HNgB. Thus, we propose that HNgB undergoes structural changes during oxidative stress and functions as a non-receptor-mediated oxidative stress-responsive sensor for neuroprotection.

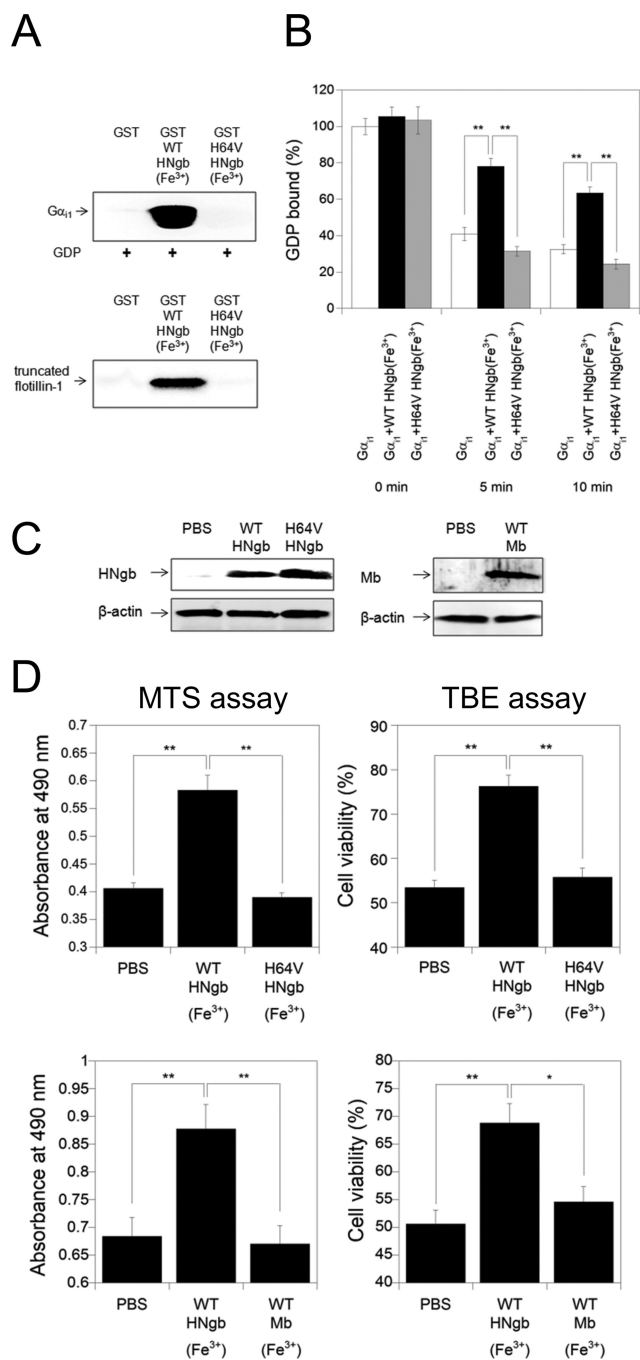
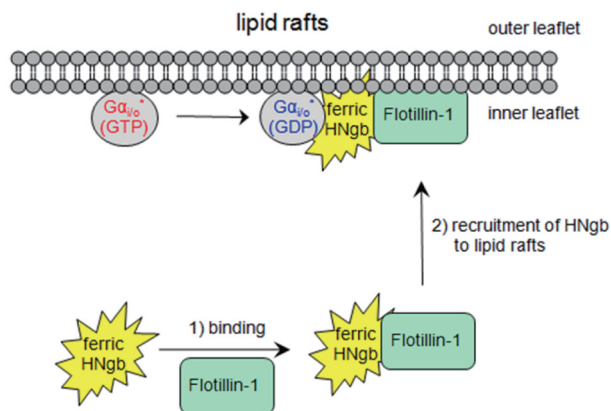


FIGURE 5. Functional analyses of the H64V HNgb mutant. A, GST pull-down assays with H64V HNgb and $G\alpha_{i1}$ or truncated flotillin-1. GST, GST-fused WT or H64V HNgb mutant was incubated with human GDP-bound $G\alpha_{i1}$ or truncated flotillin-1 in a buffer (pH 7.4). Western blot analyses were performed with anti- $G\alpha_{i1}$ mouse monoclonal antibody or with anti-flotillin-1 rabbit polyclonal antibody. B, effect of the H64V mutation on dissociation of GDP from recombinant human GDP-bound $G\alpha_{i1}$. The amount of [3 H]GDP bound to $G\alpha_{i1}$ in the absence of HNgb at 0 min was defined as 100%. All data are expressed as means \pm S.E. from four independent experiments. **, $p < 0.01$. C, Western blot analyses of PC12 cell lysates after protein transduction. PBS, WT HNgb, H64V HNgb or Mb was applied to PC12 cells with Chariot. The cells were then incubated for 3 h. Cell lysates were analyzed on 15.0% SDS/PAGE and by Western blot analyses using rabbit anti-HNgb polyclonal antibody, mouse anti- β -actin monoclonal antibody or rabbit anti-Mb polyclonal antibody. D, protective effect of WT or H64V HNgb or WT Mb on PC12 cell death induced by hypoxia/reoxygenation. WT or H64V HNgb or Mb was applied to PC12 cells with Chariot, and cell viabilities were measured by MTS and TBE assays. Data are expressed as means \pm S.E. from three independent experiments, each performed in triplicate. *, $p < 0.05$, **, $p < 0.01$.

A Oxidative stress conditions



B In the absence of HNgb

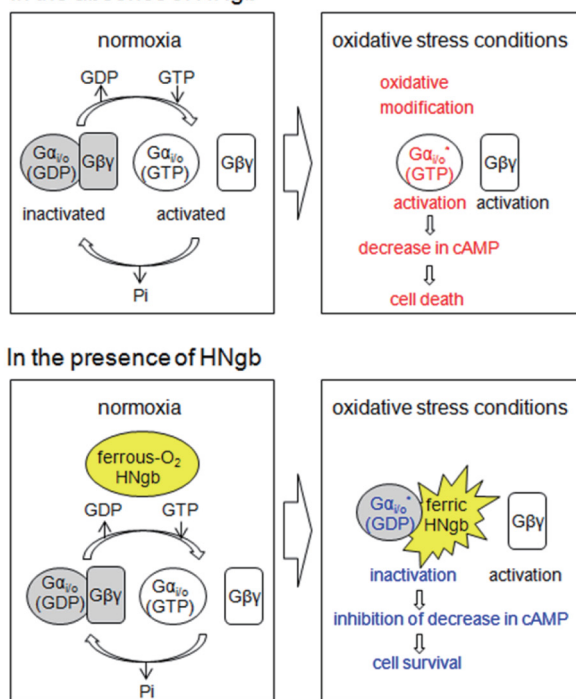


FIGURE 6. Schematic representation of the neuroprotective mechanism of HNgb. A, recruitment of HNgb to lipid rafts by specific interaction with flotillin-1 under oxidative stress conditions. B, regulation of enzymatic activity of ROS-modified $G\alpha_{i/o}$ by ferric HNgb under oxidative stress conditions.

Furthermore, we showed that ferric HNgb, but not ferric ZNgb bound to human $G\alpha_{i1}$. Previously, we generated HNgb mutants in the amino acids that differ between HNgb and ZNgb and clarified that Glu-53, Arg-97, Glu-118, and Glu-151 of HNgb are crucial for its GDI and neuroprotective activities (7, 23). By contrast, the present study showed that human flotillin-1 bound to both ferric ZNgb and ferric HNgb, suggesting that residues conserved between HNgb and ZNgb proteins are crucial for the interaction with human flotillin-1. Further studies to identify these crucial residues are now in progress.

The $G\alpha_{i/o}$ family is specifically activated by ROS produced during conditions of oxidative stress because the cysteine residues that are modified during oxidative stress are conserved only among $G\alpha_{i/o}$, and not among other $G\alpha$ families such as

$G\alpha_s$. ROS modifies $G_{i/o}$, which leads to activation of $G\alpha_{i/o}$ and dissociation into $G\alpha_{i/o}$ and $G\beta\gamma$ (Fig. 6B). Activation of $G\alpha_{i/o}$ decreases the intracellular cAMP concentration, leading to cell death (Fig. 6B). In the presence of HNgb, however, ferric bis-His HNgb is recruited to lipid rafts by interacting with flotillin-1, where it acts as a GDI for modified $G\alpha_{i/o}$, resulting in inhibition of the decrease in intracellular cAMP concentration (Fig. 6B). Thus, HNgb can protect against cell death.

The functional roles of $G\alpha_{i/o}$ and $G\alpha_s$ in cell survival or death are completely opposite (47–49). $G\alpha_s$ stimulates adenylate cyclases to activate the cAMP signaling pathway, whereas $G\alpha_{i/o}$ inhibits adenylate cyclases. The activation of G_s has been shown to increase glutathione and to protect neuronal cells against oxidative stress (49). Recently, it has been reported that $G\alpha_s$ inhibits hydrogen peroxide-induced apoptosis of SH-SY5Y cells (48); overexpression of a constitutively active $G\alpha_s$ mutant protected, while $G\alpha_s$ siRNA augmented hydrogen peroxide-induced apoptosis in SH-SY5Y cells (48). In addition, the protective effect of $G\alpha_s$ was abolished by co-expressing a constitutively active G_i mutant, which antagonizes $G\alpha_s$ by inhibiting adenylate cyclase (48). Moreover, hydrogen peroxide-induced apoptosis was reduced by treating cells with prostaglandin E_2 , which activates $G\alpha_s$, but was augmented by CCPA, which activates G_i , causing a decrease in cAMP levels (48). Furthermore, it should be also noted that a GDI and a guanine nucleotide exchange factor (GEF) of $G\alpha_{i/o}$ regulate autophagy by balancing G protein activity antagonistically (47). These data are not at all contradictory; rather, they indicate that either activation of $G\alpha_s$ or inactivation of $G\alpha_{i/o}$ leads to protection against cell death. Therefore, regulation of the $G\alpha_{i/o}$ signaling pathway by HNgb should be used as a critical step in the decision of cell survival or cell death.

Other hypotheses concerning the neuroprotective mechanism of human Ngb have been reported (50, 51). Initially, Ngb was suggested to be an O_2 storage protein similar to Mb (1). However, the low concentration (in the micromolar range) of Ngb in brain tissues except for the retina perhaps argues against a role for Ngb in storing and carrying significant amounts of O_2 . Alternatively, Ngb may act as an intracellular scavenger of ROS and/or nitric oxide (NO) (5, 52–54). It has been reported that both H64V HNgb and Mb generate very reactive cytotoxic ferryl (Fe^{4+}) species upon treatment of the ferric form with peroxide (42). In the present study, we showed that neither Mb nor H64V HNgb enhanced cell death. Moreover, our previous studies demonstrated that ZNgb and the E53Q, R97Q, E118Q, and E151N HNgb mutants, which can act as ROS scavengers by forming the bis-His conformation, do not inhibit cell death (7). Therefore, we conclude that the neuroprotective effect of human Ngb is due to its GDI activity and not to its scavenging activity against ROS.

HNgb is the first reported sensor that consists of a single globin domain alone, although some globin-coupled sensors in which globin domains are fused to methyl-accepting chemotaxis protein domains or domains for second-messenger regulation have been reported (55). It should be also noted that the function of Ngb proteins has been changing dynamically throughout the evolution of life. For example, fish Ngb has a very different function, *i.e.* a cell-membrane-penetrating activ-

ity, without the fusion of other domains (19). Further studies to investigate the function of Ngb from several different species will provide clues to not only its molecular evolutionary process but also its physiological significance.

REFERENCES

- Burmester, T., Weich, B., Reinhardt, S., and Hankeln, T. (2000) A vertebrate globin expressed in the brain. *Nature* **407**, 520–523
- Reuss, S., Saaler-Reinhardt, S., Weich, B., Wystub, S., Reuss, M. H., Burmester, T., and Hankeln, T. (2002) Expression analysis of neuroglobin mRNA in rodent tissues. *Neuroscience* **115**, 645–656
- Schmidt, M., Giessel, A., Laufs, T., Hankeln, T., Wolfrum, U., and Burmester, T. (2003) How does the eye breathe? Evidence for neuroglobin-mediated oxygen supply in the mammalian retina. *J. Biol. Chem.* **278**, 1932–1935
- Li, R. C., Morris, M. W., Lee, S. K., Pouranfar, F., Wang, Y., and Gozal, D. (2008) Neuroglobin protects PC12 cells against oxidative stress. *Brain Res.* **1190**, 159–166
- Li, R. C., Pouranfar, F., Lee, S. K., Morris, M. W., Wang, Y., and Gozal, D. (2008) Neuroglobin protects PC12 cells against β -amyloid-induced cell injury. *Neurobiol. Aging* **29**, 1815–1822
- Sun, Y., Jin, K., Mao, X. O., Zhu, Y., and Greenberg, D. A. (2001) Neuroglobin is up-regulated by and protects neurons from hypoxic-ischemic injury. *Proc. Natl. Acad. Sci. U.S.A.* **98**, 15306–15311
- Watanabe, S., and Wakasugi, K. (2008) Neuroprotective function of human neuroglobin is correlated with its guanine nucleotide dissociation inhibitor activity. *Biochem. Biophys. Res. Commun.* **369**, 695–700
- Khan, A. A., Wang, Y., Sun, Y., Mao, X. O., Xie, L., Miles, E., Graboski, J., Chen, S., Ellerby, L. M., Jin, K., and Greenberg, D. A. (2006) Neuroglobin-overexpressing transgenic mice are resistant to cerebral and myocardial ischemia. *Proc. Natl. Acad. Sci. U.S.A.* **103**, 17944–17948
- Sun, Y., Jin, K., Peel, A., Mao, X. O., Xie, L., and Greenberg, D. A. (2003) Neuroglobin protects the brain from experimental stroke *in vivo*. *Proc. Natl. Acad. Sci. U.S.A.* **100**, 3497–3500
- Dewilde, S., Kiger, L., Burmester, T., Hankeln, T., Baudin-Creuz, V., Aerts, T., Marden, M. C., Caubergs, R., and Moens, L. (2001) Biochemical characterization and ligand binding properties of neuroglobin, a novel member of the globin family. *J. Biol. Chem.* **276**, 38949–38955
- Kitatsuji, C., Kuroguchi, M., Nishimura, S., Ishimori, K., and Wakasugi, K. (2007) Molecular basis of guanine nucleotide dissociation inhibitor activity of human neuroglobin by chemical cross-linking and mass spectrometry. *J. Mol. Biol.* **368**, 150–160
- Wakasugi, K., Nakano, T., and Morishima, I. (2003) Oxidized human neuroglobin as a heterotrimeric $G\alpha$ protein guanine nucleotide dissociation inhibitor. *J. Biol. Chem.* **278**, 36505–36512
- Gilman, A. G. (1987) G proteins: transducers of receptor-generated signals. *Annu. Rev. Biochem.* **56**, 615–649
- Hepler, J. R., and Gilman, A. G. (1992) G proteins. *Trends Biol. Sci.* **17**, 383–387
- Simon, M. I., Strathmann, M. P., and Gautam, N. (1991) Diversity of G proteins in signal transduction. *Science* **252**, 802–808
- Wakasugi, K., Kitatsuji, C., and Morishima, I. (2005) Possible neuroprotective mechanism of human neuroglobin. *Ann. N.Y. Acad. Sci.* **1053**, 220–230
- Awenius, C., Hankeln, T., and Burmester, T. (2001) Neuroglobins from the zebrafish *Danio rerio* and the pufferfish *Tetraodon nigroviridis*. *Biochem. Biophys. Res. Commun.* **287**, 418–421
- Fuchs, C., Heib, V., Kiger, L., Haberkamp, M., Roesner, A., Schmidt, M., Hamdane, D., Marden, M. C., Hankeln, T., and Burmester, T. (2004) Zebrafish reveals different and conserved features of vertebrate neuroglobin gene structure, expression pattern, and ligand binding. *J. Biol. Chem.* **279**, 24116–24122
- Wakasugi, K., Takahashi, N., Uchida, H., and Watanabe, S. (2011) Species-specific functional evolution of neuroglobin. *Mar. Genomics* **4**, 137–142
- Watanabe, S., and Wakasugi, K. (2008) Zebrafish neuroglobin is a cell-membrane-penetrating globin. *Biochemistry* **47**, 5266–5270
- Watanabe, S., and Wakasugi, K. (2010) Identification of residues critical

- for the cell-membrane-penetrating activity of zebrafish neuroglobin. *FEBS Lett.* **584**, 2467–2472
22. Watanabe, S., and Wakasugi, K. (2011) Module M1 of zebrafish neuroglobin acts as a structural and functional protein building block for a cell-membrane-penetrating activity. *PLoS ONE* **6**, e16808
 23. Wakasugi, K., and Morishima, I. (2005) Identification of residues in human neuroglobin crucial for guanine nucleotide dissociation inhibitor activity. *Biochemistry* **44**, 2943–2948
 24. Wakasugi, K., Nakano, T., Kitatsuji, C., and Morishima, I. (2004) Human neuroglobin interacts with flotillin-1, a lipid raft microdomain-associated protein. *Biochem. Biophys. Res. Commun.* **318**, 453–460
 25. Bickel, P. E., Scherer, P. E., Schnitzer, J. E., Oh, P., Lisanti, M. P., and Lodish, H. F. (1997) Flotillin and epidermal surface antigen define a new family of caveolae-associated integral membrane proteins. *J. Biol. Chem.* **272**, 13793–13802
 26. Browman, D. T., Hoegg, M. B., and Robbins, S. M. (2007) The SPFH domain-containing proteins: more than lipid raft markers. *Trends Cell Biol.* **17**, 394–402
 27. Stuermer, C. A. (2009) The reggie/flotillin connection to growth. *Trends Cell Biol.* **20**, 6–13
 28. Zhao, F., Zhang, J., Liu, Y. S., Li, L., and He, Y. L. (2011) Research advances on flotillins. *Viol. J.* **8**, 479
 29. Simons, K., and Toomre, D. (2000) Lipid rafts and signal transduction. *Nat. Rev. Mol. Cell Biol.* **1**, 31–39
 30. Moffett, S., Brown, D. A., and Linder, M. E. (2000) Lipid-dependent targeting of G proteins into rafts. *J. Biol. Chem.* **275**, 2191–2198
 31. Oh, P., and Schnitzer, J. E. (2001) Segregation of heterotrimeric G proteins in cell surface microdomains. G_q binds caveolin to concentrate in caveolae, whereas G_i and G_s target lipid rafts by default. *Mol. Biol. Cell* **12**, 685–698
 32. Quinton, T. M., Kim, S., Jin, J., and Kunapuli, S. P. (2005) Lipid rafts are required in G_{α_i} signaling downstream of the P2Y₁₂ receptor during ADP-mediated platelet activation. *J. Thromb. Haemost.* **3**, 1036–1041
 33. Yuyama, K., Sekino-Suzuki, N., Sanai, Y., and Kasahara, K. (2007) Translocation of activated heterotrimeric G protein G_{α_o} to ganglioside-enriched detergent-resistant membrane rafts in developing cerebellum. *J. Biol. Chem.* **282**, 26392–26400
 34. Nishida, M., Maruyama, Y., Tanaka, R., Kontani, K., Nagao, T., and Kurose, H. (2000) $G_{\alpha_{i1}}$ and G_{α_o} are target proteins of reactive oxygen species. *Nature* **408**, 492–495
 35. Nishida, M., Schey, K. L., Takagahara, S., Kontani, K., Katada, T., Urano, Y., Nagano, T., Nagao, T., and Kurose, H. (2002) Activation mechanism of G_i and G_o by reactive oxygen species. *J. Biol. Chem.* **277**, 9036–9042
 36. Aida, Y., and Pabst, M. J. (1990) Removal of endotoxin from protein solutions by phase separation using Triton X-114. *J. Immunol. Methods* **132**, 191–195
 37. Liu, S., Tobias, R., McClure, S., Styba, G., Shi, Q., and Jackowski, G. (1997) Removal of endotoxin from recombinant protein preparations. *Clin. Biochem.* **30**, 455–463
 38. Yang, B., Oo, T. N., and Rizzo, V. (2006) Lipid rafts mediate H₂O₂ pro-survival effects in cultured endothelial cells. *FASEB J.* **20**, E688–E697
 39. Wakasugi, K., and Morishima, I. (2005) Preparation and characterization of a chimeric zebrafish-human neuroglobin engineered by module substitution. *Biochem. Biophys. Res. Commun.* **330**, 591–597
 40. Thomas, T. C., Schmidt, C. J., and Neer, E. J. (1993) G-protein α_o subunit: Mutation of conserved cysteines identifies a subunit contact surface and alters GDP affinity. *Proc. Natl. Acad. Sci. U.S.A.* **90**, 10295–10299
 41. Uno, T., Ryu, D., Tsutsumi, H., Tomisugi, Y., Ishikawa, Y., Wilkinson, A. J., Sato, H., and Hayashi, T. (2004) Residues in the distal heme pocket of neuroglobin. Implications for the multiple ligand binding steps. *J. Biol. Chem.* **279**, 5886–5893
 42. Lardinois, O. M., Tomer, K. B., Mason, R. P., and Deterding, L. J. (2008) Identification of protein radicals formed in the human neuroglobin-H₂O₂ reaction using immuno-spin trapping and mass spectrometry. *Biochemistry* **47**, 10440–10448
 43. Abramov, A. Y., Scorziello, A., and Duchen, M. R. (2007) Three distinct mechanisms generate oxygen free radicals in neurons and contribute to cell death during anoxia and reoxygenation. *J. Neurosci.* **27**, 1129–1138
 44. Morris, M. C., Depollier, J., Mery, J., Heitz, F., and Divita, G. (2001) A peptide carrier for the delivery of biologically active proteins into mammalian cells. *Nat. Biotechnol.* **19**, 1173–1176
 45. Wakasugi, K., Takahashi, N., and Watanabe, S. (2011) Chimeric ZHHH neuroglobin is a novel cell membrane-penetrating, neuroprotective agent. *Am. J. Neuroprotec. Neuroregen.* **3**, 42–47
 46. Anselmi, M., Brunori, M., Vallone, B., and Di Nola, A. (2007) Molecular dynamics simulation of deoxy and carboxy murine neuroglobin in water. *Biophys. J.* **93**, 434–441
 47. Garcia-Marcos, M., Ear, J., Farquhar, M. G., and Ghosh, P. (2011) A GDI (AGS3) and a GEF (GIV) regulate autophagy by balancing G protein activity and growth factor signals. *Mol. Biol. Cell* **22**, 673–686
 48. Kim, S. Y., Seo, M., Kim, Y., Lee, Y. I., Oh, J. M., Cho, E. A., Kang, J. S., and Juhn, Y. S. (2008) Stimulatory heterotrimeric GTP-binding protein inhibits hydrogen peroxide-induced apoptosis by repressing BAK induction in SH-SY5Y human neuroblastoma cells. *J. Biol. Chem.* **283**, 1350–1361
 49. Lewerenz, J., Letz, J., and Methner, A. (2003) Activation of stimulatory heterotrimeric G proteins increases glutathione and protects neuronal cells against oxidative stress. *J. Neurochem.* **87**, 522–531
 50. Brunori, M., and Vallone, B. (2006) A globin for the brain. *FASEB J.* **20**, 2192–2197
 51. Nienhaus, K., and Nienhaus, G. U. (2007) Searching for neuroglobin's role in the brain. *IUBMB Life* **59**, 490–497
 52. Fordel, E., Thijs, L., Martinet, W., Lenjou, M., Laufs, T., Van Bockstaele, D., Moens, L., and Dewilde, S. (2006) Neuroglobin and cytoglobin overexpression protects human SH-SY5Y neuroblastoma cells against oxidative stress-induced cell death. *Neurosci. Lett.* **410**, 146–151
 53. Fordel, E., Thijs, L., Martinet, W., Schrijvers, D., Moens, L., and Dewilde, S. (2007) Anoxia or oxygen and glucose deprivation in SH-SY5Y cells: A step closer to the unraveling of neuroglobin and cytoglobin functions. *Gene* **398**, 114–122
 54. Herold, S., Fago, A., Weber, R. E., Dewilde, S., and Moens, L. (2004) Reactivity studies of the Fe(III) and Fe(II)NO forms of human neuroglobin reveal a potential role against oxidative stress. *J. Biol. Chem.* **279**, 22841–22847
 55. Gilles-Gonzalez, M. A., and Gonzalez, G. (2005) Heme-based sensors: defining characteristics, recent developments, and regulatory hypotheses. *J. Inorg. Biochem.* **99**, 1–22